

Evolution of biofilms during the colonization process of pyrite by *Acidithiobacillus thiooxidans*

Dulce M. González · René H. Lara · Keila N. Alvarado ·
Donato Valdez-Pérez · Hugo R. Navarro-Contreras ·
Roel Cruz · Jessica Viridiana García-Meza

Received: 23 February 2011 / Revised: 22 April 2011 / Accepted: 25 April 2011 / Published online: 20 July 2011
© Springer-Verlag 2011

Abstract We have applied epifluorescence principles, atomic force microscopy, and Raman studies to the analysis of the colonization process of pyrite (FeS_2) by sulfuroxidizing bacteria *Acidithiobacillus thiooxidans* after 1, 15, 24, and 72 h. For the stages examined, we present results comprising the evolution of biofilms, speciation of $\text{S}_n^{2-}/\text{S}^0$ species, adhesion forces of attached cells, production and secretion of extracellular polymeric substances (EPS), and its biochemical composition. After 1 h, highly dispersed attached cells in the surface of the mineral were observed. The results suggest initial non-covalent, weak interactions (e.g., van der Waal's, hydrophobic interactions), mediating an irreversible binding mechanism to electrooxidized massive pyrite electrode (eMPE), wherein the initial production of EPS by individual cells is determinant. The mineral surface reached its maximum cell cover between 15 to 24 h. Longer biooxidation times resulted in the

progressive biofilm reduction on the mineral surface. Quantification of attached cell adhesion forces indicated a strong initial mechanism (8.4 nN), whereas subsequent stages of mineral colonization indicated stability of biofilms and of the adhesion force to an average of 4.2 nN. A variable EPS (polysaccharides, lipids, and proteins) secretion at all stages was found; thus, different architectural conformation of the biofilms was observed during 120 h. The main EPS produced were lipopolysaccharides which may increase the hydrophobicity of *A. thiooxidans* biofilms. The highest amount of lipopolysaccharides occurred between 15–72 h. In contrast with abiotic surfaces, the progressive depletion of $\text{S}_n^{2-}/\text{S}^0$ was observed on biotic eMPE surfaces, indicating consumption of surface sulfur species. All observations indicated a dynamic biooxidation mechanism of pyrite by *A. thiooxidans*, where the biofilms stability and composition seems to occur independently from surface sulfur species depletion.

D. M. González · R. H. Lara · R. Cruz · J. V. García-Meza (✉)
Geomicrobiology, Institute of Metallurgy, UASLP,
Sierra Leona 550, Lomas 2°,
78210 San Luis Potosí, SLP, Mexico
e-mail: jvgm@uaslp.mx

K. N. Alvarado
Basics Sciences Laboratory, UASLP,
Salvador Nava 110,
78210 SLP, Mexico

D. Valdez-Pérez
Institute of Physics, UASLP,
Salvador Nava 110,
78210 SLP, Mexico

H. R. Navarro-Contreras
CIACyT, UASLP,
Sierra Leona 550, Lomas 2°,
78210 SLP, Mexico

Keywords *Acidithiobacillus thiooxidans* · Pyrite · Biofilms evolution · Electrooxidation · Interfacial analysis · Proteins quantification

Introduction

Interfacial mechanisms describing the development of leaching bacterial biofilms on mineral sulfides (SM) are of great significance for determining the bioleaching pathways of SM. The sulfur-oxidizing microorganisms (SOM: Archaea or Bacteria) play a major role in the cycling of sulfur in the biosphere. SOM processed surface sulfur species (e.g., elemental sulfur, S^0 ; polysulfides, S_n^{2-}) as a source of energy and reducing power; this metabolic capability has been applied in the mining industry for the bioleaching of metals

from SM, since SOM as *Acidithiobacillus thiooxidans* and *Acidithiobacillus caldus* may oxidize the intermediary sulfur species released after the iron has been oxidized by iron-oxidizing microorganisms (IOMs, e.g., *Leptospirillum ferrooxidans*) (Rawlings et al. 1999; Dopson and Lindström 1999). SOM also provide protons (bioacidification) to maintain Fe(III) in its oxidized state (Schipper and Sand 1999). The former explained why S^0 was generally added to promote the growth of *A. thiooxidans* in some bioleaching process where mixed populations of leaching bacteria are added (Liu et al. 2008). The degradation of an acid-insoluble SM as pyrite (FeS_2) arises via the thiosulfate mechanism by means of electron extraction, by the indirect attack of hydrated Fe(III) ions from the crystal lattice. The main reduced sulfur obtained is the thiosulfate, which via a series of reactions subsequently yields sulfate and protons (via tetrathionate and other polythionates) or S^0 (Schipper and Sand 1999). S^0 is produced in significant amounts (10–20%) during the chemical or electrochemical oxidation of pyrite at pH <2, moderate temperature and pressure, and in absence of SOM (Hamilton and Wood 1981; Schipper and Sand 1999; Rohwerder et al. 2003); thus, S^0 generated may act as a barrier against the diffusion of oxygen or Fe(III) ions, affecting global SM reactivity, and delaying the complete oxidation process of SM (Mustin et al. 1993; Dopson and Lindström 1999; Fowler and Crundwell 1999; Bevilaqua et al. 2002; Nava et al. 2008). Several researches indicated that the attachment of cells as biofilms to SM surfaces enhances bioleaching of SM (Pogliani and Donati 1999; Sand et al. 2001; Rodríguez et al. 2003; Sharma et al. 2003). A biofilm is a highly organized system of microorganisms, embedded in a self-produced, gelatinous, and highly hydrated matrix, composed of extracellular polymeric substances (EPS; comprise 50–90% of the biofilm), ions, gases, colloidal and particulate compounds, and open water channels. Thus, the EPS of biofilms constitute an interfacial matrix or media between the cell membrane and the mineral surface whereon the microorganisms are attached and the chemical mineral transformations occur. The importance of the composition of such matrix during the microorganisms/substratum interaction is evidenced in the fact that, e.g., attached cells of the SOM *A. thiooxidans* growing in sulfur produce up to 85–100 times more EPS than planktonic cells (Harneit et al. 2006; Lara et al. 2010). According to Sand, Gehrke, and collaborators, the biofilm matrix of IOMs represents a reactive space wherein the electrochemical mechanisms/surface reaction takes place, since EPS-complexed Fe(III) ions interacts with the pyrite surface by electrostatic interactions, and just this EPS-complexed Fe(III) performed the oxidative attack of SM, through a “contact mechanism” (Kinzler et al. 2003; Rohwerder and Sand 2007). However, the researchers also suggested that SOM completely lack complexed Fe(III) or other positive

charged groups in their EPS, but relies on other different mechanisms in addition to electrostatic forces (Rohwerder et al. 2003); possibly, through molecularly mediated specific EPS and outer membrane proteins, e.g., the adhesins (Chi et al. 2007; Chandraprabha et al. 2010), or by pili-mediated bond to the mineral surface, as was observed for *Acidithiobacillus ferrooxidans* (Li et al. 2010).

A previous work applying on electrooxidized pyrite indicated that *A. thiooxidans* forms a monolayered biofilm after 5 days of inoculation, wherein the contact resulted in a strong adhesion force (0.467 nN) between the cells and the altered surface (Lara et al. 2010). The results suggested that *A. thiooxidans* attaches directly to the electrooxidized pyrite surface during the dynamic interfacial mechanisms of S^0 biooxidation. *A. thiooxidans* attachment does not require EPS-complexed Fe(III) ions because the biooxidation of the elemental S^0 to sulfate may occur via enzymatic catalysis, e.g., the sulfur-dioxygenase or sulfur oxygenase (catalyzing the oxidation of S^0 to sulfite, HSO_3^-) and a sulfite acceptor oxidoreductase or dehydrogenase (HSO_3^- to SO_4^{2-}) (Kelly 1985; Schipper and Sand 1999; Rother et al. 2001; Rohwerder and Sand 2007). Direct contact of *A. thiooxidans* on the pyrite surface was previously suggested (Takakuwa et al. 1977; Konishi et al. 1995; Fowler and Crundwell 1999; Liu et al. 2003) and reported in pure and mixed cultures of *A. thiooxidans* (Florian et al. 2009; Echeverría and Demergasso 2009). For the studies on the interfacial processes of biofilm colonization and biooxidative attack of SM, a set of combined methods has been proposed; e.g., atomic force microscopy (AFM), epifluorescence microscopy, and Raman spectroscopy (Mangold et al. 2008a, b; Edwards et al. 1999).

In our earlier work, we studied biofilms of the SOM *A. thiooxidans* on previously electrooxidized pyrite surfaces (electrooxidized massive pyrite electrode, eMPE), analyzing the role of EPS during cells attachment, the adhesion forces implied, and the status of surface sulfur species during biooxidation processes; these analysis were done using confocal laser scanning microscopy (CLSM), AFM, and Raman spectroscopy, respectively (Lara et al. 2010). We used eMPE because (1) major biofilm was established on the eMPE after biotic assays rather than in the chemically altered MPE, and (2) allows a better development of the insoluble sulfur species, defined by the AFM analysis and easily identified by Raman spectroscopy. Now, the aims of this new work are twofold: first, to describe the interfacial changes of pyrite during the evolution of biofilms in the mineral colonization process by *A. thiooxidans*; and second, to reexamine the role of bacterial EPS during contact mechanisms between this SOM and pyrite during the evolution, analyzing the biochemical components of EPS during the different stages of S_n^{2-}/S^0 species biooxidation.

Materials and methods

Mineral samples

Pyrite samples were obtained from Zacatecas, Mexico. The sampled pyrite purity is of ~99.5% wt, with minor amounts of chalcopyrite (CuFeS_2 , 0.3% wt) and sphalerite (ZnS , 0.5% wt), according with mineralogical analysis performed after chemical analysis of total acid-digested samples, X-ray diffraction patterns, and scanning electron microscopy coupled to energy dispersive X-ray spectroscopy analyses. Crystals of pyrite were selected for the construction of massive pyrite electrodes (MPE). These MPE were mineral sections of 1.2–1.5 cm^2 , mounted in epoxy resin with a silver epoxy electrical contact on the backside. The MPE pristine surface (un-oxidized) was polished until mirror-like polishing surfaces are reached.

Potentiostatic oxidation of massive pyrite electrodes (eMPE)

Electrooxidation of MPE allows the overproduction of both S^0 and S_n^{2-} species directly from the pyrite under acidic conditions (Mycroft et al. 1990; Lara et al. 2010). Thus, the MPE surfaces were electrochemically oxidized according with Lara et al. (2010), in acidified (pH 2) ATCC-125 (American Type Culture Collection) growing medium. The selected potential for these experiments was 1.11 V/SHE (during 3,600 s); using an autolab PGSTAT 30 coupled to a PC and a classic Pyrex® glass three electrode cell. Hence, the working electrode was the MPE, the counter electrode was a graphite rod (Alfa Aesar, 99.9995% purity), and the reference electrode was a saturated sulfate electrode (SSE, 0.615 V vs. The standard hydrogen electrode, SHE). Consequently, the formation of $\text{S}_n^{2-}/\text{S}^0$ species on eMPE surfaces was confirmed by Raman spectroscopy after each electrooxidation of MPE.

Bacterial strain and cultivation

The strain ATCC-8085 of *A. thiooxidans* was used in this study. The microorganism was cultivated aerobically, until the exponential growth phase (~ 10^8 cells/mL) at 28–30°C in 50 mL of media ATCC-125 is reached, which per liter of distilled water contained: 10 g of S^0 , 3 g of KH_2PO_4 , 0.4 g of $(\text{NH}_4)_2\text{SO}_4$, 0.5 g of $\text{MgSO}_4 \cdot 7\text{H}_2\text{O}$, 0.25 g of $\text{CaCl}_2 \cdot 2\text{H}_2\text{O}$, and 0.01 g of $\text{FeSO}_4 \cdot 7\text{H}_2\text{O}$. The media was dispensed into 250-mL Erlenmeyer flasks and were sterilized by autoclaving at 121°C for 15 min. The S^0 was sterilized separately using 2–3 h of UV irradiation; the sterilization was done spreading carefully the S^0 over a crystal surface, in an active laminar (horizontal) flow cabinet; and every hour, the dispersed S^0 was shaken in

order to homogenize the exposure of S^0 grains. Final pH of medium was adjusted to 2 with H_2SO_4 . A planktonic (suspended) inoculum was used for the biotic experiments.

Biofilms formation

Because $\text{S}_n^{2-}/\text{S}^0$ species are required to sustain the metabolic activity of the SOM *A. thiooxidans*, eMPE surfaces were used as the source of $\text{S}^0/\text{S}_n^{2-}$ species, as it was described in previous studies (Lara et al. 2010): eMPE surfaces were sterilized by exposing to UV irradiation for 2 h; afterward, the eMPE was placed in a flask with 100 mL of the ATCC-125 at pH 2 without none S^0 source, and with ~ 10^8 cells/mL of *A. thiooxidans*. The culture was incubated aerobically at 28–30°C and 150 rpm during 1, 15, 24, and 72 h. These biotic assays were done in triplicate. An “abiotic” (uninoculated) control was also carried out in triplicate to compare between chemical and biological oxidation of $\text{S}^0/\text{S}_n^{2-}$. After each time, the resulted eMPEs were collected, dried with a direct current of nitrogen, and preserved in a desiccator under inert conditions until their analysis.

Quantification of proteins and polysaccharides in EPS of biofilms

Quantification of proteins and polysaccharides composing the EPS after 1, 15, 24, 72, and 120 h of microorganism colonization was carried out using the well-known Bradford (1976) and Dubois (1959) methods, respectively. Each biotic eMPE was spoiled using a bistoury set to remove biofilms; eppendorf vials were used to collect cells under iced conditions (4°C). Vials were left inundated with 300 μL of acidified ATCC-125 medium or 1,150 μL of saline solution (NaCl, 2%), according with protocols for proteins and polysaccharides extraction methods, respectively. For EPS extraction, different eluents (NaCl, NaOH, Na_2EDTA , and the culture media) were assayed, and the stain Alcian Blue (specific for polysaccharides) to check the extraction efficiency of each eluent, according to Barranguet et al. (2004). The NaCl showed the highest extraction efficiency of bacterial EPS from cells, at concentration of 2%. For the Bradford method, vials were centrifuged during 15 min (5,000 rpm), whereas 20 min (14,000 rpm) were allowed for the Dubois method. Temperature was controlled during these procedures of extraction (4°C). Pellets were resuspended using 300 μL of acidified ATCC-125 medium or phenol solution (5%) for washing procedures, according with proteins and polysaccharides analysis, respectively. Bradford reaction was promoted by adding 3 mL of Bradford reagent into vials and mixed until reach homogeneous solutions. Dubois reaction was promoted by adding 2.5 mL of H_2SO_4 in vials, followed by 15 min

of ambient temperature. Subsequently, vials were placed in water bath during 15 min (30°C). Proteins and carbohydrates quantification was carried out by comparing UV measurements (UV-Visible Spectrophotometer 50 Bio) with a reference curve, constructed under similar conditions of analysis. The polysaccharide concentration in the samples was determined by comparing the measured absorption values with those of a calibration range of fresh α -glucose standards of known concentrations between 1 and 100 mg/mL. Albumin was used as standards of protein of known concentrations between 1 and 30 mg/mL. All materials and solutions were previously sterilized by autoclaving and/or UV irradiation.

Surface analysis of eMPEs

eMPE's surfaces were analyzed by AFM, CLSM, and Raman spectroscopy to evaluate the evolution of interfacial processes associated with four stages of mineral colonization by *A. thiooxidans*. Before the essays, observations and analysis of MPE were carried out for pristine (un-electrooxidized) and electrooxidized surfaces (previous to immersion in ATCC-125). After 1, 15, 24, and 72 h of bioassay, the same analyses were done for biotic (eMPE immersed in culture media with *A. thiooxidans*) and abiotic control (eMPE in culture media without *A. thiooxidans*).

The AFM analysis of MPE and eMPEs was performed with a Nanoscope Multimode IIIa digital instrument. Narrow and wide regions were visualized to obtain topographic images by the tapping mode (scan rate between 0.5 and 1 Hz). At least, images of 30 regions per MPE surface were obtained. The silicon cantilever showed a free resonance frequency between 275 and 325 kHz and a constant between 31.18 and 44.53 N/m during these experiments. Force separation curves were acquired using contact mode sampling 1 μm^2 areas in order to quantify the adhesion forces of attached cells in biofilms. At least 400 curves were taken from each specific surface, and 10% of the obtained curves were randomly analyzed. The Si_3N_4 cantilever showed a free resonance frequency between 90 and 115 kHz and a constant between 1.08 and 2.03 N/m during the collection of these curves. Additionally, roughness (R_a , nm) and root mean square (R_q , nm) of eMPEs were also evaluated in each specific surface.

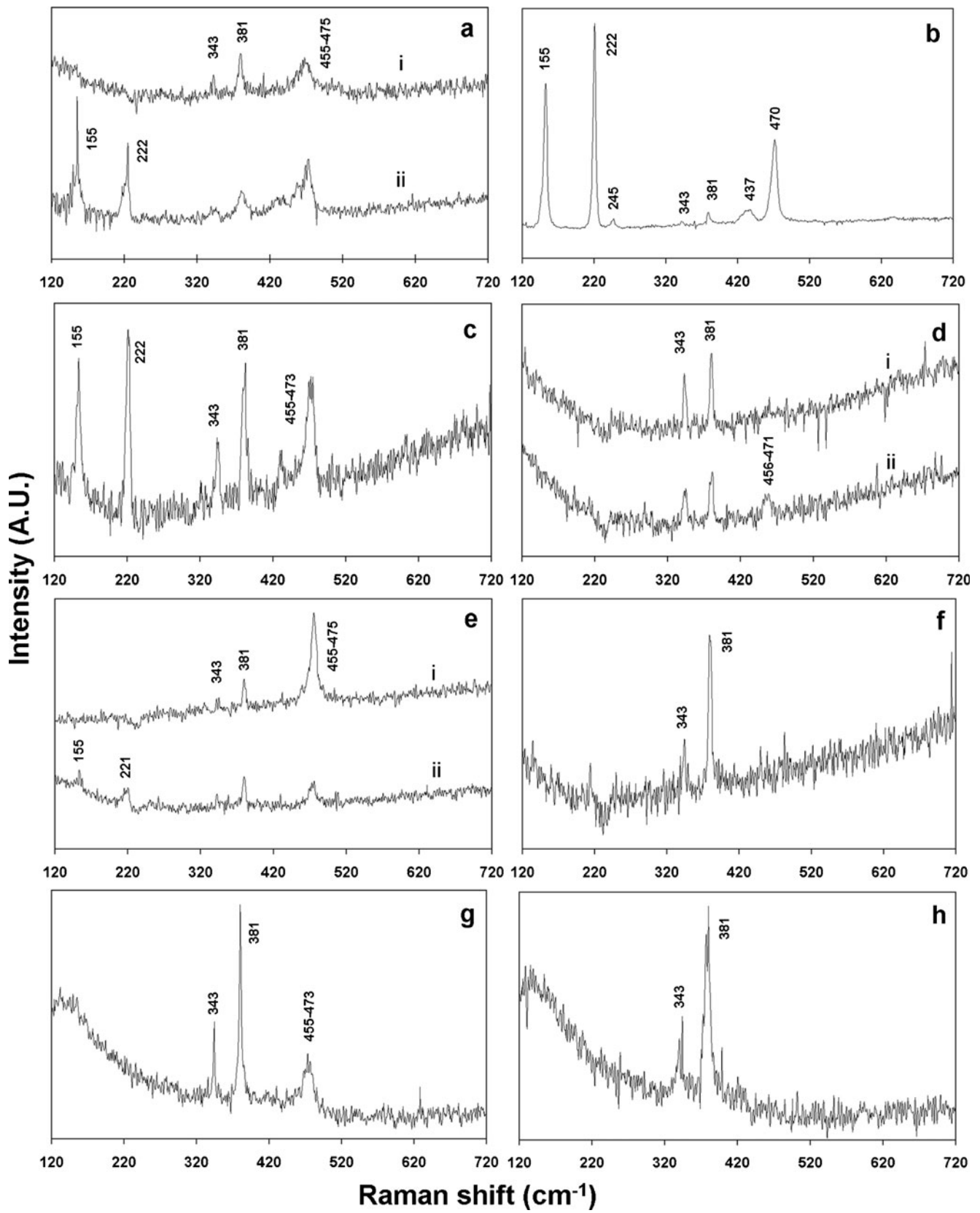
After AFM analysis, the same eMPEs exposed to *A. thiooxidans* (biotic surfaces) were analyzed by CLSM. The biofilms were previously fixed with two to three drops of formaldehyde (3%), stained during 30 min in the dark using lectin *Canavalia ensiformis* (Con-A; tetramethylrhodamine conjugated; Molecular Probes, Eugene, OR, USA) and the lipophilic fluorescent stain Nile Red (NR; Sigma Aldrich) were used to stain polysaccharides (α -mannose and α -

glucose) and hydrophobic domains (as lipids) composing EPS, respectively. Several drops of 0.1 g/L of Con-A solution were added to the MPE's surface, and after 75 min of incubation at 30°C under dark conditions, the MPE's surface was rinsed with HEPES (N-2-hydroxyethylpiperazine-N9-2-ethanesulfonic acid, at 10 mM and pH 7.4) buffer. Immediately after staining with Con-A, several drops of NR at 10% in ethanol (w/v) were added to the MPE and after 10 min at 30°C in the dark, the MPE's surface was rinsed again with HEPES. This process was applied for eMPE's surfaces obtained for the different stages of mineral colonization. Planktonic cells of *A. thiooxidans* were also stained, for comparison purposes. The planktonic cells from the culture media were smeared on a slide by capillary action within a sterile loop; immediately, the cells were fixed with formaldehyde and stained as was described previously. After cells staining, the eMPE's surfaces and the slide for planktonic cells were examined using a CLSM (Leica DMI4000B) using a $\times 63$ immersion objective. CLSM images were acquired in 2D. Con-A was excited at 488 nm and the emitted signal was detected using a band pass filter for emission at 575 nm; NR was excited 515–560 nm; emission, >590 nm. The relative signal intensity of three groups in depth was resolved using the software program of the CLSM (Leica LAS AF). The data were corrected for background signal.

The intensity of Con-A and NR fluorescence was used to estimate the relative contribution of extracellular polysaccharides (stained with Con-A) and lipids (stained with NR) to biofilm; the data were expressed in Arbitrary units (A.U.). It has been demonstrated that CLSM is useful for quantify EPS in biofilms (Zhang and Fang 2001) and that CLSM is more sensitive than the chemical extraction of EPS in young and less compact biofilms (Barranguet et al. 2004); however, an underestimation of EPS by CLSM occurred for >35 μm thick and larger compact biofilms.

Finally, Raman spectroscopy analysis was carried out in pristine MPE, in electrooxidized MPE, in electrooxidized MPE after the biotic and the abiotic assays, and in the non-electrooxidized MPE exposed to the culture media without *A. thiooxidans*. A triple monochromator Raman Jobin Yvon T64000 spectrometer equipped with an optical microscope (Olympus BH2-UMA) was used. The detector was a charged coupled device cooled by liquid nitrogen. MPE's surfaces were excited by an Ar^+ laser beam at 514 nm

Fig. 1 Raman spectra collected on abiotic control and biooxidized eMPE surfaces: **a, c, e, g** are control abiotic surfaces after 1, 15, 24, and 72 h of immersion, respectively (without exposition to *A. thiooxidans* cells); **b, d, f, h** are biooxidized surfaces after 1, 15, 24, and 72 h of inoculation with *A. thiooxidans*. Some altered surfaces involve two types of mineral zones, as indicated by *i* and *ii*, according with abundance of Raman spectra collected therein. Sixty seconds of collection time, $\lambda=514$ nm



(Stabilité 2017, Spectra Physics) with a power of 2 mW, and focused with a diameter of about 0.8 μm on the sample. Collection time was 60 s in each analysis. At least ten Raman spectra were collected from each specific surface. Raman performance and calibration was validated using a Si wafer by observing the well-known Si LO single sharp peak at 521 cm^{-1} . Raman backscattering showed a signal/noise ratio greater than 100 for Si analysis, ensuring a good Raman performance during mineral surface analysis (Lara et al. 2010). The vibrational range analyzed was 100–750 cm^{-1} , as the $\text{S}^0/\text{S}_n^{2-}$ species show their main active modes within this interval (e.g., Sasaki et al. 1998; Toniazzi et al. 1999).

Results

Raman analysis was carried out in order to evaluate the sulfur speciation on eMPE's surfaces during abiotic and biotic trials after 1, 15, 24, and 72 h of trial (Fig. 1). In all cases, Raman peaks at 343 (ν_2) and 381 (ν_1) cm^{-1} typically indicated pristine pyrite surfaces (e.g., Sasaki et al. 1998). Additionally, in the abiotic control, and after 1 h, the presence of $\text{S}^0/\text{S}_n^{2-}$ species were confirmed because the associated Raman peaks at 155 (ν_2), 222 (ν_3), and 455–475 (ν_1 ; Fig. 1a) (Mycroft et al. 1990; Sasaki et al. 1998; Toniazzi et al. 1999) are now visible. This fact indicated the formation of two mixed sulfur-rich areas, where the presence of S^0 seems to be more abundant than S_n^{2-} (diverse polysulfide species), accordingly with the suggested abundance from the frequency of appearance of the Raman spectra for S^0 species collected in such areas (Fig. 1a, ii).

After 15 h, Raman spectra collected from the abiotic control indicated a better crystallization of S^0 and minor amounts of S_n^{2-} , since Raman peaks at 155, 222, and 455–473 cm^{-1} (this last with some asymmetry) are sharp and well defined (Fig. 1c); in contrast, Raman spectra collected after 24 h showed mostly an intense sharp peak at 455–475 cm^{-1} indicating the formation of S_n^{2-} species in most of oxidized mineral areas (Fig. 1e, i); however, minor amounts of $\text{S}^0/\text{S}_n^{2-}$ species were also identified (Fig. 1e, ii), according with the presence of additional Raman peaks at 155 and 221 cm^{-1} (Fig. 1e) (Mycroft et al. 1990).

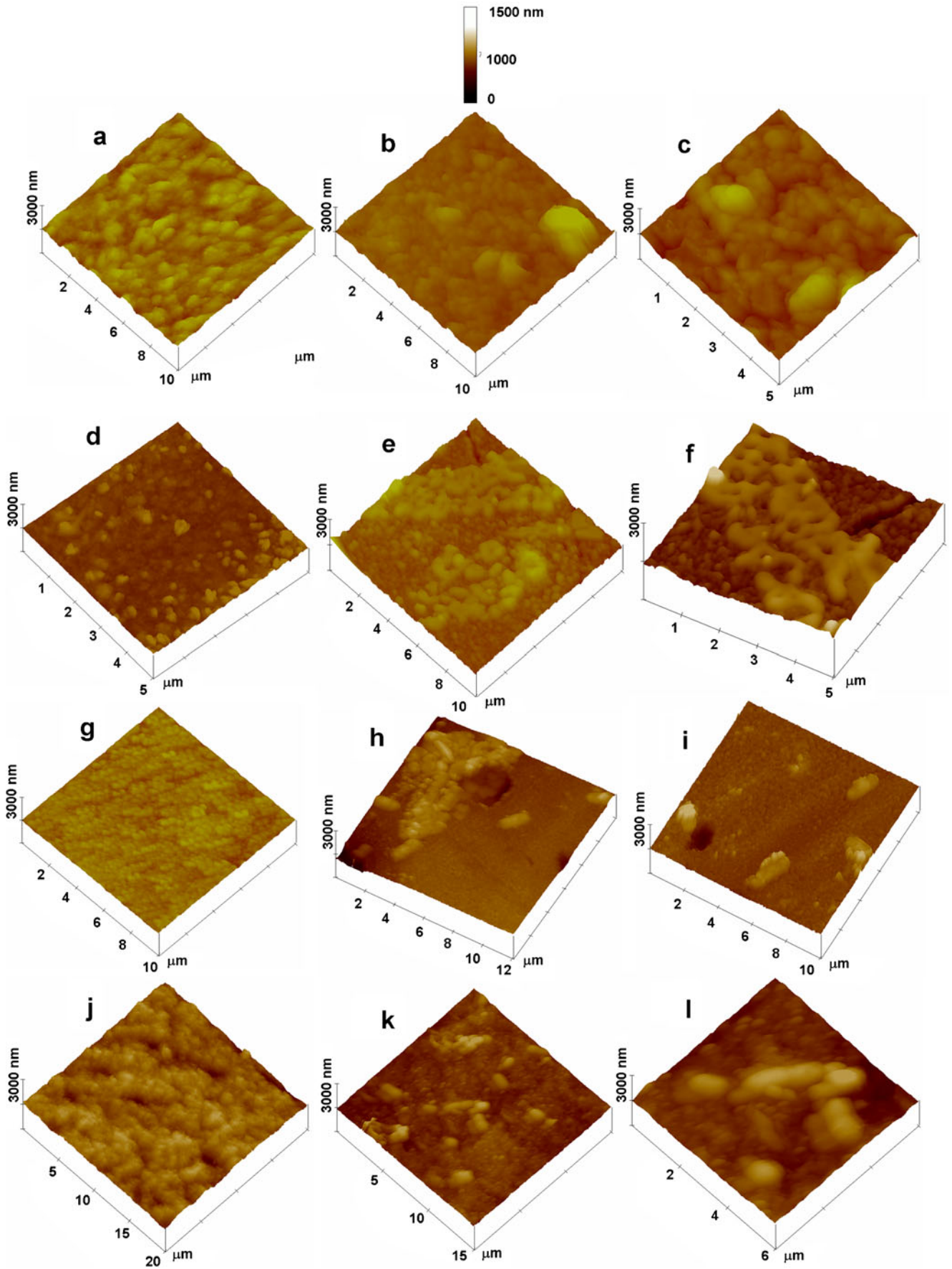
Finally, analysis collected after 72 h of the abiotic control indicated exclusively the formation of S_n^{2-} species, (Fig. 1g). The Raman results discussed above suggested a cyclic formation of variable amounts of $\text{S}^0/\text{S}_n^{2-}$ species on the altered pyrite, restricted by kinetic processes only. Some S^0 species are progressively oxidized to sulfate ions, whereas S_n^{2-} produced S^0 due to oxidizing conditions in acidic medium. The stability of low amounts of $\text{S}^0/\text{S}_n^{2-}$

species (10–20%) during chemical oxidation of pyrite in acidic conditions has been indicated by Schippers and Sand (1999). Other authors have pointed out the presence of $\text{S}^0/\text{S}_n^{2-}$ species after chemical or electrochemical oxidation of pyrite, under acidic conditions (Mycroft et al. 1990; Sasaki et al. 1998). Consequently, the eMPEs here prepared are adequate interfaces for inducing the mineral colonization by sulfur-oxidizing *A. thiooxidans* cells.

The Raman spectra for the eMPE's surfaces in the biotic trials after 1, 15, 24, and 72 h, are presented in Fig. 1b, d, f, and h, respectively. Surprisingly, the Raman spectra collected after 1 h indicated the clear formation of very-well-crystallized S^0 species, according with sharp peaks at 155, 222, and 470 cm^{-1} , as well as minor peaks at 245 and 437 cm^{-1} also for the S^0 species (Fig. 1b). The precedent results can be indicative of initial stage of $\text{S}^0/\text{S}_n^{2-}$ biooxidation, and that a modification of the crystalline structure of $\text{S}^0/\text{S}_n^{2-}$ seems to occur, in agreement with AFM observations (Fig. 2b, areas surrounding attached cells). After 15 h different altered mineral zones were observed, some with S_n^{2-} species (Fig. 1d, ii) and others with a total depletion of sulfur species (Fig. 1d, i); these results suggested the progressive $\text{S}^0/\text{S}_n^{2-}$ consumption during the first 15 h, by *A. thiooxidans*. Finally, after 24 and 72 h of biotic assay, no peaks for reduced sulfur species were observed (Fig. 1f, h), indicating the total depletion or consumption of $\text{S}^0/\text{S}_n^{2-}$ species.

After Raman study, similar eMPE's surfaces were analyzed by AFM (Fig. 2). Figure 2a, d, g, and j shows images collected from control (abiotic) surfaces after 1, 15, 24, and 72 h, respectively. These surfaces had a similar Ra, as a result of the formation of the nanoscale size structures of $\text{S}^0/\text{S}_n^{2-}$; thus, changes in their structure aggregation and shape (e.g., Fig. 2a, d) could be associated with the variable crystallization degree achieved during the $\text{S}^0/\text{S}_n^{2-}$ chemical alteration. The former results are in agreement with the cyclic generation–consumption behavior of $\text{S}^0/\text{S}_n^{2-}$, as seen by the Raman study discussed above, at different stages of eMPE's immersion in acidic ATCC-125 medium. Figure 2b, c, e, f, h, i, k, and l shows images collected from biotic surfaces after 1, 15, 24, and 72 h of biooxidation. Here, eMPE's surfaces suggested variable amounts of attached cells. After 1 h, there were few clusters (Fig. 2b, c). This fact is in agreement with Ra and Rq values obtained for

Fig. 2 Three dimension images of AFM from abiotic control and biooxidized eMPE surfaces: **a, d, g, j** are images from control surfaces after 1, 15, 24, and 72 h of immersion, respectively (without exposition to *A. thiooxidans* cells); **b, c, e, f, h, i, k, l** are images from biooxidized surfaces after 1, 15, 24, and 72 h of inoculation with *A. thiooxidans* cells. Images were acquired in air using tapping mode and a scan rate of 0.5–1 Hz. Height of elements is shown on figure



eMPE's surfaces after 1 h (biotic, areas surrounding attached cells; or abiotic) there were no significant variations in these observed parameters (Table 1), thus indicating limited S^0/S_n^{2-} consumption associated with the scant bacterial–mineral colonization at this stage. Nevertheless, the small differences observed in shape between the nanoscale size structures in biotic (Fig. 2a) and abiotic (Fig. 2b) surfaces seems to be associated with better crystallization of S^0 species in biotic surfaces, in agreement with the Raman study (Fig. 1b).

After 15 h of biooxidation, cluster of attached cells may be observed (Fig. 2e, f). In general overview, Ra and Rq values (Table 1), as well as Raman results confirmed the occurrence of S^0/S_n^{2-} biooxidation during the biological activity of *A. thiooxidans*, and they are a clear evidence that illustrates the progressive depletion of S^0/S_n^{2-} on altered pyrite surfaces, during evolution of mineral colonization.

In order to achieve a complete description of interfacial mechanisms associated with cells attachment, the adhesion forces was obtained for the identified stages of mineral colonization. After 1 h, the adhesion force of biofilms was 8.1 nN, whereas at longer times of biooxidation was 4.1, 3.92, and 5.43 nN for 15, 24, and 72 h, respectively (Fig. 3).

Former studies were completed by CLSM analysis to analyze the presence and development of biofilms on the

eMPE, as the AFM images suggested. Images collected from planktonic (suspended) cells (Fig. 4a) and 120 h of biooxidation (Fig. 4f) were also included for comparison purposes. CLSM study confirmed the presence of clusters of attached cells (1 h, Fig. 4b) and the formation of monolayered biofilms (15 and 24 h, Fig. 4c and d); however, at 120 h (Fig. 4f), CLSM study confirmed the progressive decrease of biofilms, and only dispersed attached cells were observed (Fig. 4e).

Epifluorescence analysis indicated variable secretion of extracellular polysaccharides and lipids (as hydrophobic domains) for the stages associated with biofilms evolution (Table 2). After 1 h of biooxidation, significant differences of EPS production were found (at a significance level of $p < 0.05$ for $n=28$) between cells forming biofilm and free (planktonic) cells; actually, 5.32 times more exopolysaccharides and 1.23 times more lipids, comparing with the planktonic (suspended) cells. Longer times of biooxidation implies changes in the quantity of these EPS, and the maximum secretion of exopolysaccharides and lipids were achieved at 72 and 24 h, respectively. The higher secretion of EPS was not observed to be associated with the intensity of the strength of the cell attachment, i.e., in the initial adhesion stages, where the strongest adhesion force was measured (Fig. 3), is far from the maximum EPS expression.

Table 1 Evolution of root mean square (Rq) and roughness (Ra) values collected for stages found of biofilms evolution collected on eMPE areas

MPE surface	Area ($\mu\text{m} \times \mu\text{m}$)	Number of areas	RMS (Rq), nm	Roughness (Ra), nm
Electrooxidized (1.11 V/SHE)	5×5	5	24.35±2.18	19.41±1.78
	1×1	35	22.85±2.15	18.25±1.66
Abiotic assay (1 h)	5×5	27	70.01±5.98	56.34±4.45
	1×1	34	51.79±10.17	42.30±8.89
Biotic assays (1 h, collected on top of attached cells)	5×5	5	89.33±11.88	64.95±7.89
	1×1	14	59.40±18.22	46.99±15.71
Abiotic assay (15 h)	5×5	25	64.96±15.67	46.24±7.13
	1×1	34	45.13±11.09	37.29±4.24
Biotic assays (15 h, surrounding attached cells)	5×5	14	57.07±8.56	35.27±9.91
	1×1	25	40.32±13.27	32.18±10.54
Abiotic assay (24 h)	5×5	30	71.05±23.97	55.38±8.22
	1×1	40	47.12±13.29	39.66±7.12
Biotic assays (24 h, surrounding attached cells)	5×5	17	24.80±6.93	18.16±5.68
	1×1	33	16.10±4.94	12.57±3.82
Abiotic assay (72 h)	5×5	34	58.55±9.55	46.72±7.09
	1×1	27	41.40±8.96	33.35±7.22
Biotic assays (72 h, surrounding attached cells)	5×5	9	29.61±5.38	23.15±3.99
	1×1	16	25.65±3.64	20.74±3.25
Abiotic assay (120 h)	5×5	50	83.77±9.78	66.97±8.32
	1×1	25	80.54±4.12	62.56±3.25
Biotic assays (120 h, surrounding attached cells)	5×5	25	45.13±3.58	36.08±3.01
	1×1	45	37.41±4.83	30.27±4.72

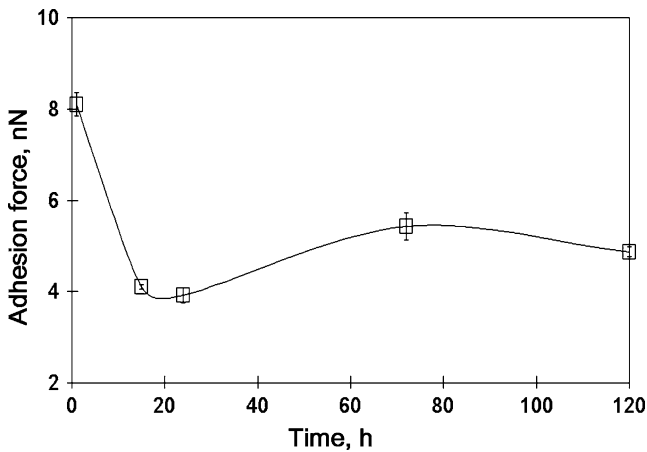


Fig. 3 Adhesion forces of attached *A. thiooxidans* cells as a function of the biooxidation time; adhesion forces were acquired in air using AFM contact mode (scan rate of 0.5–1 Hz), $n=3$

Quantification of extracellular proteins and polysaccharides completed the understanding of the biofilm compositions for the different stages found in the biofilm evolution (Table 3). A progressive increase for extracellular proteins

Table 2 Epifluorescence values in planktonic and cells composing biofilms for the stages found in mineral colonization

Time (h)	Polysaccharides A.U.		Lipids A.U.	
	Free cells	Biofilms	Free cells	Biofilms
1	2.34	12.48 (5.32)	33.38	41.07 (1.23)
15	2.23	28.52 (12.77)	26.46	107.69 (4.09)
24	5.45	72.19 (13.22)	16.49	102.24 (6.19)
72	2.37	40.91 (17.26)	32.90	129.86 (3.94)
120	2.33	32.89 (14.09)	34.60	32.45 (0.93)

$n=28.52$ (12.77)50. Times for over expression of extracellular polysaccharides and lipids in each stage, with respect to the planktonic cells (indicated in parentheses)

and polysaccharides content was found; the lowest concentration was recorded at the first hour, while the highest concentration, was achieved at 72 h (2.47 and 10.54 mg/L, respectively; Table 3). Significant differences of EPS production (at a significance level of $p<0.05$ for $n=3$) during each time were found, except for extracellular proteins at 15 and 24 h.

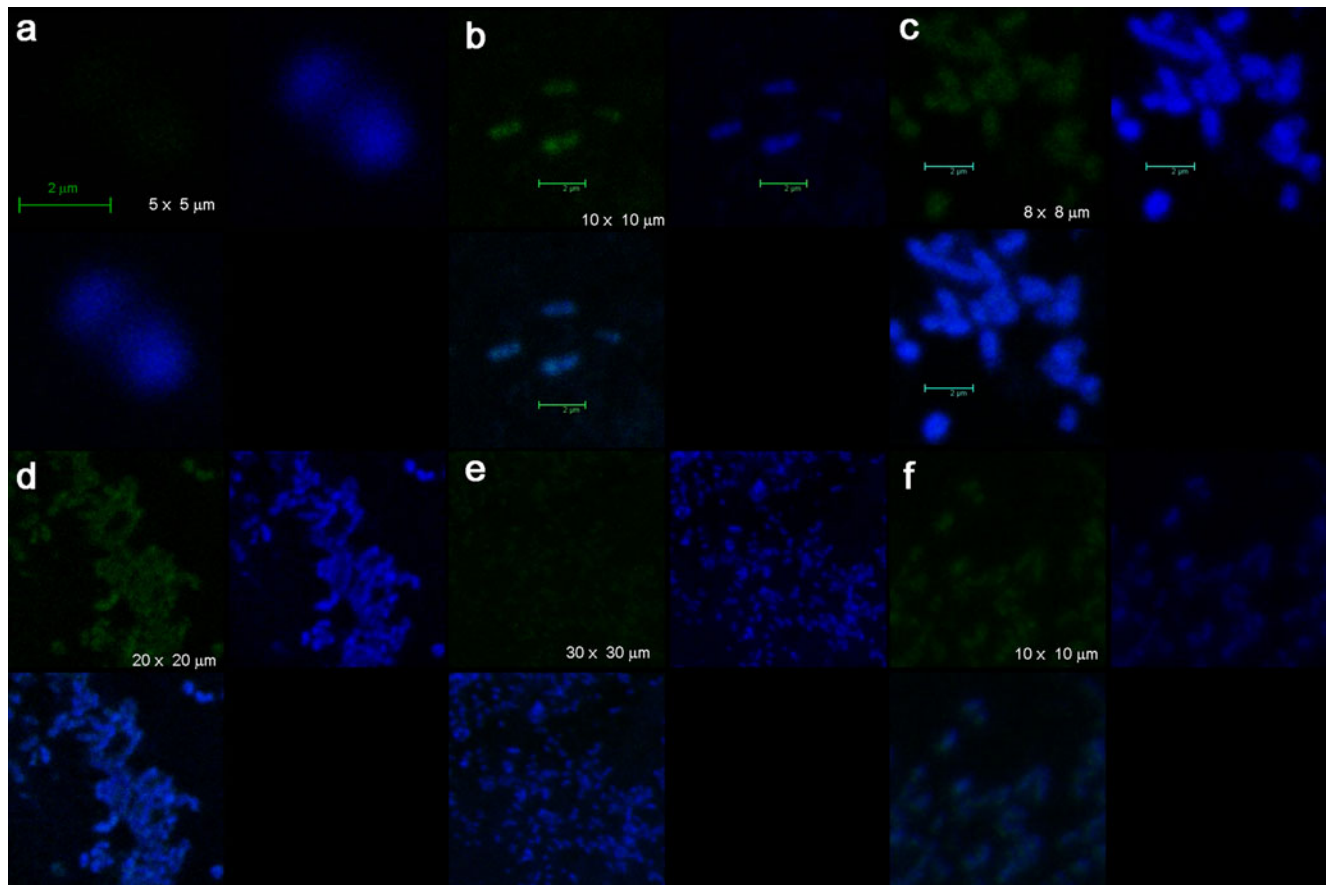


Fig. 4 CLSM images of *A. thiooxidans* cells (2D): **a** planktonic (suspended) cells; after biooxidation of eMPE’s surfaces at: **b** 1 h, **c** 15 h, **d** 24 h, **e** 72 h, and **f** 120 h. Epifluorescence of exopolysaccharides

is in *green*, whereas lipids is in *blue*. An overlap of both epifluorescence images is presented in the lower left side of images (**a** to **f**)

Table 3 Quantification of extracellular proteins and polysaccharides for the stages found in mineral colonization

Time (h)	Proteins		Polysaccharides	
	Absorbance	mg/mL	Absorbance	mg/mL
0	0.002	0.031	0.003	0.17
1	0.034	0.596	0.016	1.29
15	0.043	1.37	0.067	4.94
24	0.043	1.416	0.075	5.52
72	0.055	2.473	0.145	10.54
120	0.029	0.14	0.036	2.77

n=3

Discussion

A. thiooxidans forms biofilms strongly attached to the surface of the MPE previously electrooxidized (eMPE), suggesting an intimate physical contact between the bacteria and the pyrite, which resulted in strong adhesion forces (range, 3.92–8.10 nN; Table 1). The colonization initiated after 1 h, consisting of clusters attached cells onto the surface of the mineral (Fig. 2). This initial contact resulted in the strongest adhesion force recorded through the biofilm assay (8.1 nN). Subsequently longer colonization times resulted in stability of attached cells and the changes in biofilms adhesion forces were negligible (Fig. 3).

At initial time, the minimal EPS production and secretion was recorded but its results were significantly higher than the EPS of planktonic cells ($p < 0.05$ for $n = 28$). An increase in EPS content is directly associated with the increase of epifluorescence in attached cells, reflecting considerable EPS thickness (Fig. 4); the data of epifluorescence indicated that EPS mainly comprise hydrophobic domains (as lipids; Table 2). The aforementioned results suggest initial non-covalent, weak interactions, mediating an irreversible binding mechanism to eMPE, wherein the initial production of EPS by individual cells is determinant. The former was supported by experimental data of different authors in systems with *A. ferrooxidans*: (a) the attached cells to pyrite are more hydrophobic than suspended ones; the hydrophobicity brings down the interfacial tension between cells and the surface of sulfur or pyrite, to enhance contact and adhesion (Devasia et al. 1993; Devasia and Natarajan 2010); and (b) the attachment of the cells to hydrophobic substrata as pyrite and sulfur is dominated by van der Waal's attraction forces (Gehrke et al. 1998). Thus, hydrophobicity helps in adhesion (Donlan 2002).

After 15 h, the number of cells significantly increased and a biofilm with a monolayer structure was observed; later, ca. the 24th hour, a biofilm with two layers of cells

was observed. A concomitant increase of the EPS production was recorded between the 15th and before the 120th hour (Tables 2 and 3). This highest content of EPS is related with the increase of the cell number but also with the establishment of a self-covered matrix of EPS in biofilms, as it was observed during CLSM studies and suggested during the AFM studies.

It has been demonstrated that the nature and quantity of EPS produced and secreted by bioleaching cells is strongly influenced by the culture conditions and the electrochemical characteristics of the substratum (Donlan 2002), and that free-living (planktonic) cells produce less EPS than cell attached to a mineral (Harneit and Sand 2007); also, that the main EPS produced by bioleaching microorganisms grown on pyrite are neutral polysaccharides (glucose, rhamnose, fucose, xylose, and mannose), lipids or saturated fatty acids, and lipopolysaccharides (Gehrke et al. 1998).

Interestingly, our results showed the dominance of hydrophobic domains (as extracellular lipids) in the EPS of both, the free and biofilm-forming cells of *A. thiooxidans*, with a maximum within the 15–72 h (Tables 2 and 3). Elevated level of lipids is closely associated with the late stages of biofilm maturation in *Mycobacterium tuberculosis* (Ojha et al. 2005) and lipids and lipopolysaccharides are essential for the biofilm adhesive stability under extreme environmental conditions. Previous report indicated that when *A. ferrooxidans* grew attached on sulfur or pyrite produced more lipids (Vu et al. 2009) and that lipopolysaccharide may be a prerequisite for such attachment (Gehrke et al. 1998). Apparently, lipids enhance elemental sulfur oxidation acting as a wetting agent (Beebe and Umbreit 1971). Yet, the high content of lipids increases the hydrophobicity of *A. thiooxidans* biofilms. Since S^0 is also hydrophobic, the sulfur–cell interaction is hydrophobic. Because lipids and hydrophobic domains strongly influence lipid-mediated adhesion mechanisms in biofilm, it is necessary to investigate the effect of surfactants or the hydrophobicity of EPS in suspensions, by measuring liquid–liquid partition in aqueous and organic phase using.

Devasia et al. (1993) and Devasia and Natarajan (2010) distinguish proteinaceous compounds on the surface of *A. ferrooxidans* attached to pyrite, and conclude that an induction of relatively hydrophobic proteins is required for adhesion, changes the cell surface chemistry and hence the utilization of sulfur, and is also a prerequisite for exopolysaccharides secretion.

Thus, extracellular polysaccharides and lipids play a key role in cell adherence, favoring hydrophobic interaction, but also extracellular or surface proteins are involved in adhesion and are linked to electron transport; both are key aspects in bacterial colonization and oxidation of insoluble substrates (Bobadilla et al. 2011). The initial stage of cell attachment involves the highest adhesion force but also the

smallest extracellular protein concentration (Table 3); this fact cannot be fully explored in the present work. However, it may be explained invoking the fact that adhesines are important molecules involved in any bacterial adhesion process, and in our case it may proceed as follows: an extracellular (outer membrane) 40-KDa protein was described by Jerez et al. (1992), such protein named Omp40 participates in the adhesion of *A. ferrooxidans* to hydrophobic sulfur aggregates (Arredondo et al. 1994). It is hypothesized that the secretion of an “Omp40-like” protein by *A. thiooxidans* (Bobadilla et al. 2011) also occurs. Additionally, and more important, Ohmura et al. (1996) observed that the flagellum of *A. ferrooxidans* contains a 40-KDa protein which could adhere to elemental sulfur, mediated by the disulfide bond between thiol groups in the protein and elemental sulfur. More recently, Li et al. (2010) concluded that *A. ferrooxidans* colonizes and forms microcolonies on pyrite by assessing pili-mediated twitching motility and a strong adherence; such pili present the protein adhesin at its tip (Pointon et al. 2010). Pili are present in diverse groups of bacteria, but no studies on pilis and adhesines of *A. thiooxidans* have been performed yet. This process could be also implied at initial adhesion of *A. thiooxidans* cells to pyrite; however, such important question should be clarified in subsequent work. However, another piece of information that may be related with the adhesion process is the fact that Bobadilla et al. (2011) reported the major secreted protein by *A. thiooxidans* cultured with elemental sulfur, the lipoprotein *Licanantase*, which seems to be related with the colonization and oxidation of sulfur.

We propose that *A. thiooxidans* cells follow four stages during the colonization of the eMPE (of 1.2–1.5 cm²): (1) an initial hydrophobic interaction with the sulfur and the colonization of cell clusters throughout the surface; (2) the cells attached to the surface achieved a stable adhesion force and the EPS production and secretion resulted in a colony of one layer of cells; (3) the mineral surface reached its maximum cells covering sometime around 15–24 h; but the well-structured S_n²⁻/S⁰ species recorded after 1 h of biotic assay are totally depleted after 24 h (Fig. 1f, h); this starvation conditions and the high cell density, promote the transition from surface-attached cells into a mature biofilm (Figs. 2e, f, h and 4d, e); (4) at the final stage (120 h), the number cells and the quantity of EPS of the biofilms decreased and the biofilm dissolves releasing cells; the individual cells may colonize other surfaces (Monods and O’Toole 2009). During the colonization of the eMPE’s surface, cells of *A. thiooxidans* progressively biooxidized the reduced sulfur species (S_n²⁻/S⁰) of the eMPE, modifying the crystalline topography or texture of the surface structure of S_n²⁻/S⁰ as the AFM (Fig. 2) and Raman (Fig. 1) observations suggested and indicated, respectively.

Since in this experiment, the Fe(II)/Fe(III) ratio was the same in both cultures with *A. thiooxidans* and in the abiotic control (0.01 g of iron; see **Bacterial strain and cultivation**), the aforementioned results indicated that the observed differences are clearly a consequence of the oxidation of the S⁰ generated on the electrooxidized MPE by the biological activity of *A. thiooxidans*, and that S⁰ is stable during pyrite weathering in acidic conditions (abiotic assays). No passive layer was detected. The previous result is of industrial interest, since in absence of a sulfur-oxidizing microorganisms as *A. thiooxidans* large amounts of jarosite and elemental sulfur may be produced during other biochemical leaching processes, and the biofilm formed may be embedded by the jarosite deposition, as is observed by Lei et al. (2009) during the biooxidation process of chalcopyrite by *A. ferrooxidans*. Also Li et al. (2010) reported an accumulation of secondary minerals that surrounded or partially encapsulated the *A. ferrooxidans* cells; such secondary minerals modified the oxidation process of pyrite.

Acknowledgments Financial support for this work comes from the Mexican Council of Science and Technology (CONACyT; project no. 05-49321). The authors thank Dr. Amauri Pozos and Dr. Jaime Ruiz-García for access to the CLSM (Basics Sciences Laboratory) and the AFM (Colloids and Interfaces Laboratory) equipment at UASLP, respectively. The authors also thank Erasmo Mata-Martinez for mineral section preparation, Francisco Galindo-Murillo for MPE preparation. René Lara also thanks CONACyT for his postdoctoral fellowship.

References

- Arredondo R, García A, Jerez CA (1994) Partial removal of lipopolysaccharide from *Thiobacillus ferrooxidans* affects its adhesion to solids. *Appl Environ Microbiol* 60:2846–2851
- Barranguet C, van Bausekom SAM, Veuger B, Neu TR, Manders EMM, Sinke JJ, Admiraal W (2004) Studying undisturbed phototrophic biofilms: still a technical challenge. *Aquat Microbiol Ecol* 34:1–9
- Beebe JL, Umbreit WW (1971) Extracellular lipid of *Thiobacillus thiooxidans*. *J Bacteriol* 108(1):612–614
- Bevilaqua D, Leite ALLC, García O, Tuovinen OH (2002) Oxidation of chalcopyrite by *Acidithiobacillus ferrooxidans* and *Acidithiobacillus thiooxidans* in shake flask. *Process Biochem* 38:587–594
- Bobadilla RA, Levican G, Parada P (2011) *Acidithiobacillus thiooxidans* secretome containing a newly described lipoprotein *Licanantase* enhances chalcopyrite bioleaching rate. *Appl Microbiol Biotechnol* 89:771–780
- Bradford MM (1976) A rapid and sensitive method for the quantitation of microgram quantities of protein utilizing the principle of protein-dye binding. *Ann Biochem* 72:248–254
- Chandraprabha MN, Somasundaran P, Natarajan KA (2010) Modeling and analysis of nanoscale interaction forces between *Acidithiobacillus ferrooxidans* and AFM tip. *Coll Surf B Biointerfaces* 75(1):310–318
- Chi A, Valenzuela L, Beard S, Mackey AJ, Shabanowitz J, Hunt DF, Jerez CA (2007) Periplasmic proteins of the extremophile

- Acidithiobacillus ferrooxidans*. Mol Cell Proteomics 6:2239–2251
- Devasia P, Natarajan KA (2010) Adhesion of *Acidithiobacillus ferrooxidans* to mineral surfaces. Int J Miner Proces 94:135–139
- Devasia P, Natarajan KA, Sathyanarayana DN, Rao GR (1993) Surface chemistry of *Thiobacillus ferrooxidans* relevant to adhesion on mineral surfaces. Appl Environ Microbiol 59:4051–4055
- Donlan MR (2002) Biofilms: microbial life on surfaces. Emerg Infect Dis 8(9):881–890
- Dopson M, Lindström EB (1999) Potential role of *Thiobacillus caldus* in arsenopyrite bioleaching. Appl Environ Microbiol 65(1):36–40
- Dubois M (1959) Colorimetric method for determination of sugars and related substances. Anal Chem 28:350–356
- Echeverría A, Demergasso C (2009) Assessment of microbial adhesion in mixed cultures to sulfide minerals using CARD-FISH techniques. Adv Mat Reser Biohydrometallurgy 71–73:83–86
- Edwards KJ, Goebel BM, Rodgers TM, Schrenk MO, Gihring TM, Cardona MM, Hu B, McGuire MM, Hamers RJ, Pace NR, Banfield JF (1999) Geomicrobiology of pyrite (FeS₂) dissolution: case study at Iron Mountain, California. Geomicrobiol J 16:155–179
- Florian B, Noël N, Sand W (2009) Biofilm of lithotrophic leaching bacteria visualized by combined epifluorescence and atomic force microscopy. Proceedings 5th ASM Conference in Biofilms 144
- Fowler TA, Crundwell FK (1999) Leaching of zinc sulfide by *Thiobacillus ferrooxidans*: bacterial oxidation of the sulfur product layer increases the rate of zinc sulfide dissolution at high concentration of ferrous ions. Appl Environ Microbiol 65(12):5285–5292
- Gehrke T, Telegdi J, Thierry D, Sand W (1998) Importance of extracellular polymeric substances from *Thiobacillus ferrooxidans* for bioleaching. Appl Environ Microbiol 64:2743–2747
- Hamilton IC, Wood R (1981) An investigation of surface oxidation of pyrite and pyrhotite by linear potential sweep voltammetry. J Electroanal Chem 118:327–343
- Harneit K, Sand W (2007) Influence of growth substrate and attachment substratum on EPS and biofilms formation by *Acidithiobacillus ferrooxidans* A2. Adv Mat Res 20–21:385
- Harneit K, Göksel A, Kock D, Klock JH, Gehrke T, Sand W (2006) Adhesion to metal sulfide surfaces by cells of *Acidithiobacillus ferrooxidans*, *Acidithiobacillus thiooxidans* and *Leptospirillum ferrooxidans*. Hydrometallurgy 83:245–254
- Jerez CA, Seeger M, Amaro AM (1992) Phosphate starvation affects the synthesis of outer membrane proteins in *Thiobacillus ferrooxidans*. FEMS Microbiol Lett 98:29–34
- Kelly DP (1985) Physiology of the thiobacilli: elucidating the sulphur oxidation pathway. Microbiol Sci 2:105–109
- Kinzler K, Gehrke T, Telegdi J, Sand W (2003) Bioleaching: a result of interfacial processes caused by extracellular polymeric substances (EPS). Hydrometallurgy 71:83–88
- Konishi Y, Asai S, Yoshida N (1995) Growth kinetics of *Thiobacillus thiooxidans* on the surface of elemental sulfur. Appl Environ Microbiol 61(10):3617–3622
- Lara RH, Valdez-Pérez D, Rodríguez AG, Navarro-Contreras HR, Cruz R, García-Meza JV (2010) Interfacial insights of pyrite colonized by *Acidithiobacillus thiooxidans* cells under acidic conditions. Hydrometallurgy 103:35–44
- Lei J, Huaiyang Z, Xiaotong P, Zhonghao D (2009) The use of microscopy techniques to analyze microbial biofilms of the bio-oxidized chalcopyrite surface. Mineral Eng 22:37–42
- Li YQ, Wan DS, Huang SS, Leng FF, Yan L, Ni YTQ, Li HY (2010) Type IV pili of *Acidithiobacillus ferrooxidans* are necessary for sliding, twitching motility, and adherence. Curr Microbiol 60:17–24
- Liu HL, Chen BY, Lan YW, Cheng YC (2003) SEM and AFM images of pyrite surfaces after bioleaching by the indigenous *Thiobacillus thiooxidans*. Appl Microbiol Biotechnol 62:414–420
- Liu Y-G, Zhou M, Zeng G-M, Wang X, Li X, Fan T, Xu W-H (2008) Bioleaching of heavy metals from mine tailings by indigenous sulfur-oxidizing bacteria: effects of substrate concentration. Bioresour Technol 99:4124–4129
- Mangold S, Harneit K, Rohwerder T, Claus G, Sand W (2008a) Novel combination of atomic force microscopy and epifluorescence microscopy for visualization of leaching bacteria on pyrite. Appl Environ Microbiol 74(2):410–415
- Mangold S, Laxander M, Harneit K, Rohwerder T, Claus G, Sand W (2008b) Visualization of *Acidithiobacillus ferrooxidans* biofilms on pyrite by atomic force and epifluorescence microscopy under various experimental conditions. Hydrometallurgy 94:127–132
- Monods RD, O'Toole GA (2009) The developmental model of microbial biofilms: ten years of a paradigm up for review. Trends Microbiol 17(2):73–87
- Mustin C, de Donato Ph, Berthelin J, Marion Ph (1993) Surface sulphur as promoting agent of pyrite leaching by *Thiobacillus ferrooxidans*. FEMS Microbiol Rev 11(1–3):71–74
- Mycroft JR, Bancroft GM, McIntyre NS, Lorimer JW, Hill IR (1990) Detection of sulphur and polysulphides on electrochemically oxidized pyrite surfaces by X-ray photoelectron spectroscopy and Raman spectroscopy. J Electroanal Chem 292:139–152
- Nava D, González I, Leinen D, Ramos-Barrado JR (2008) Surface characterization by X-ray photoelectron spectroscopy and cyclic voltammetry of products formed during the potentiostatic reduction of chalcopyrite. Electrochem Acta 53:4889–4899
- Ohmura N, Tsugita K, Koizumi J-I, Saiki H (1996) Sulfur-binding protein of flagella of *Thiobacillus ferrooxidans*. J Bacteriol 178(19):5776–5780
- Ojha A, Anand M, Bhatt A, Kremer L, Jacobs W, Hatfull GF (2005) GroEL1: a dedicated chaperone involved in mycolic acid biosynthesis during biofilms formation in mycobacteria. Cell 123:861–873
- Pogliani C, Donati E (1999) The role of exopolymers in bioleaching of a non-ferrous metal sulphide. J Ind Microbiol Biotechnol 22(2):88–92
- Pointon JA, Smith WD, Saalbach G, Crow A, Kehoe MA, Banfield MJ (2010) Highly unusual thioester bond in a pilus adhesin is required for efficient host cell interaction. J Biol Chem 285:33858–33866
- Rawlins DE, Tributsch H, Hansford GS (1999) Reasons why '*Leptospirillum*'-like species rather than *Thiobacillus ferrooxidans* are the dominant iron-oxidizing bacteria in many commercial processes for the biooxidation of pyrite and related ores. Microbiol 145:5–13
- Rodríguez Y, Ballester A, Blázquez ML, González F, Muñoz JA (2003) New information on the pyrite bioleaching mechanisms at low and high temperature. Hydrometallurgy 71:37–46
- Rohwerder T, Sand W (2007) Mechanisms and biochemical fundamentals of bacterial metal sulfide oxidation. In: Donati ER, Sand W (eds) Microbial processing of metal sulfides. Springer, New York, pp 35–58
- Rohwerder T, Gehrke T, Kinzler K, Sand W (2003) Bioleaching review part A Progress in bioleaching: fundamentals and mechanisms of bacterial metal sulfide oxidation. Appl Microbiol Biotechnol 63:239–248
- Rother D, Henrich HJ, Quentmeier A, Bardischewsky F, Friedrich CG (2001) Novel genes of the sox gene cluster, mutagenesis of the flavoprotein SoxF, and evidence for a general sulfur-oxidizing system in *Paracoccus pantotrophus* GB17. J Bacteriol 183:4499–4508
- Sand W, Gehrke T, Jozsa P-G, Schippers A (2001) (Bio)chemistry of bacterial leaching-direct vs. indirect bioleaching. Hydrometallurgy 59:159–175

- Sasaki K, Tsunekawa M, Ohtsuka T, Konno H (1998) The role of sulfur-oxidizing bacteria *Thiobacillus thiooxidans* in pyrite weathering. *Coll Surf A* 133:269–278
- Schippers A, Sand W (1999) Bacterial leaching of metal sulfides proceeds by two indirect mechanisms via thiosulfate or via polysulfides and sulfur. *Appl Environ Microbiol* 65(1):319–321
- Sharma PK, Das A, Hanumantha Rao K, Forsberg KSE (2003) Surface characterization of *Acidithiobacillus ferrooxidans* cells grown under different conditions. *Hydrometallurgy* 71:285–292
- Takakuwa S, Nishikawa T, Hosoda K, Tominaga N, Iwasaki H (1977) Promoting effect of molybdate on the growth of a sulfur oxidizing bacterium, *Thiobacillus thiooxidans*. *J Gen Appl Microbiol* 23:163–173
- Toniazzo V, Mustin C, Portal JM, Humbert B, Benoit R, Erre R (1999) Elemental sulfur at the pyrite surfaces: speciation and quantification. *Appl Surf Sci* 143:229–237
- Vu B, Chen M, Crawford RJ, Ivanova EP (2009) Bacterial extracellular polysaccharides involved in biofilms formation. *Molecules* 14(7):2535–2554
- Zhang T, Fang HHP (2001) Quantification of extracellular polymeric substances in biofilms by confocal laser scanning microscopy. *Biotechnol Lett* 23:405–409